COMPARISON OF STRAIN MEASUREMENT METHODS ON GANYMEDE GROOVED TERRAIN: DEFORMED CRATERS VS. FAULT GEOMETRY. R. L. Michaud and G. C. Collins, Wheaton College, Norton MA 02766, michaud_robert@wheatonma.edu, gcollins@wheatonma.edu.

Introduction: One of the crucial pieces of information for understanding the tectonics of Jupiter's largest moon Ganymede is the amount of surface strain represented by the bright grooved terrain. Pappalardo and Collins [1] quantified strain based on extension of craters deformed by grooved terrain, but of course this technique was only applicable in the few places where craters are cut by faults, and not in the vast majority of other groove areas. Fault geometry had been used to quantify strain in an area with high resolution stereo coverage by Collins et al. [2], but a miniscule amount of the surface of Ganymede is covered by such data. We attempt to bridge the gap by using fault geometry techniques of strain estimation on the faults that cut strained craters, to see if the techniques provide similar answers. If so, we can use fault geometry techniques in other areas without stereo coverage to estimate strain in many more areas of Ganymede grooved terrain.

Areas Examined: We examined the same five craters as Collins and Pappalardo [1]. (a) Saltu, within dark terrain of Nicholson Regio. (b) Unnamed crater in dark terrain of Marius Regio, near Anshar Sulcus. (c) A pair of strained craters, east of Arbela Sulcus. (d) Nefertum, within grooved terrain of Nun Sulci. (e) Erichthonius, east of Erech Sulcus. We also examined an additional area with no strained craters, at the boundary of Nicholson Regio and Harpagia Sulcus (imaged at high resolution by Galileo in orbit G28).

Method for tilt-block normal faults: The faults that cut craters a-d all appear to be tilt-block normal faults (Fig. 1), common in some areas of grooved terrain [3]. The ridges we see in images of these craters are multiple fault blocks. In order to derive a strain value using the geometric method with fault blocks, we measure the proportion between the two halves of each fault block, the back tilted face (y) and the fault scarp (x) (Fig. 2). The angle θ describes the dip angle of the normal faults. This value is unknown, but we attempted to constrain it by measuring the complementary angle at the top of the ridge. Geise et al. [4] published topographic profiles of our Harpagia Sulcus target area. Assuming that the slopes at the top of the ridges have not been extensively modified, we were able to refine our approximate that $\theta = 45°$.

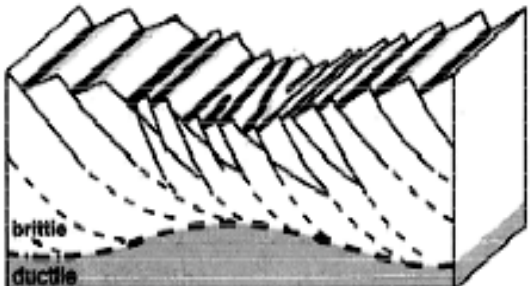

Figure 1: Schematic cross-section of tilt-block faults on Ganymede

In images of our study areas, we traced the crest of each ridge, i.e. where the top of one half of the fault block ends and where the other half begins. We also carefully mapped the bottom of each trough between the ridges, which is the closest approximation to the location of the fault (though this is sometimes complicated by material shed into the bottom of the valley). For each fault block in our target areas, we used the traced ridge top and valley bottoms to measure x and y along approximately 10-15 perpendicular lines (Fig. 3). From these measurements, we found a single representative width for each half of the fault block. Using the proportion between both slopes, along with our θ, we could find φ, the slope of the back-tilted face.

$$\frac{y}{x} = \frac{\tan(\theta-\phi)}{\tan\phi}$$

However, the equation above assumes that what we see in our images is exactly what we would see if we were directly above the surface of Ganymede. This is not usually the case - the spacecraft rarely took images directly overhead, and so we need to correct for the direction (sub s/c azimuth) and angle (emission angle) that the craft was at when it took the images. That correction was a geometric relation between the observed vs. actual lengths of the fault blocks:

$$\frac{y'}{x'} = \frac{\cos(\alpha-\phi)\sin(\theta-\phi)}{\sin\phi\cos(\theta+\alpha-\phi)}$$

where $\alpha = \theta\sin\beta$, and β is the difference in angle between the trend of the grooves and the sub-spacecraft angle. The result of this correction gives us a more accurate value for φ, which was then used in our strain equation to give us a strain value.

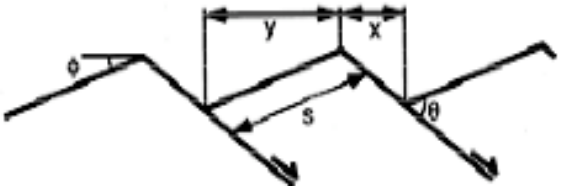

Figure 2: Relationship of y, x, and θ to the tilt blocks.

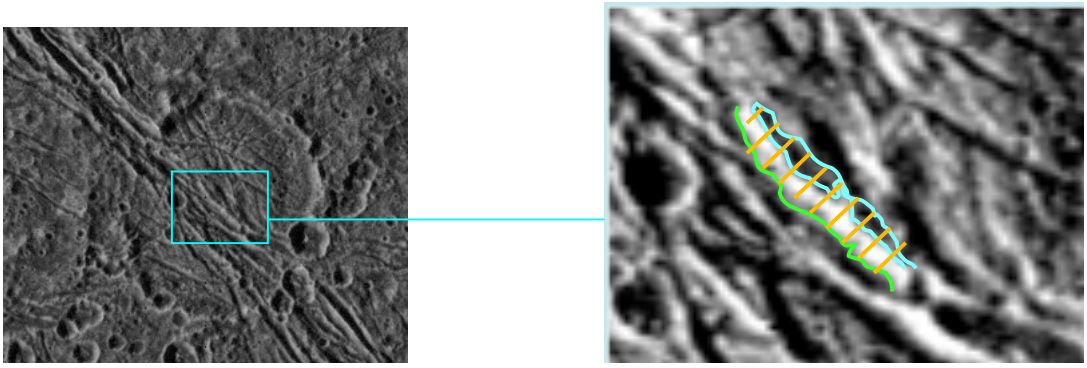

Fig. 3: Left image shows unnamed crater b in Marius Regio. Right image shows a sample fault block, with traced y (blue) and x (green) slopes measured from the crest of the ridge (center blue line), and 10 width measurement lines (orange).

$$\varepsilon = \frac{\sin\theta}{\sin(\theta-\phi)} - 1$$

The entire process was typically repeated for 10-20 fault blocks within each crater, and 52 fault blocks in the case of the Nicholson-Harpagia boundary area. Errors on the strain measurements are based on a standard deviation of all y/x values, which in turn compensates for the variations in φ.

Method for graben: In the crater Erichthonius, the faults within the crater exhibit graben morphology instead of tilt-blocks. To calculate extension in this case, we simply measured the two projected fault scarp widths, A and B, using a similar method we used for tilt-block measurement. However here we assumed φ to be constant, at 30°. Once A and B were calculated we added them together and then subtracted that total from the total observed crater length, which in turn gave us a value of crater length before the extension. The ratio between the original crater length (L_{orig}) and the extended length (L_{obs}) gave us percent extension.

$$L_{orig} = L_{obs} - A_{obs} - B_{obs}; \quad Ext_{\%} = \left(1 - \left(\frac{L_{orig}}{L_{obs}}\right)\right) \cdot 100$$

Results: Our fault geometry based strain estimates fall within the error bars of the values reported by Pappalardo and Collins [1] using an entirely independent technique. It is important to point out that the reported strain value for crater b was actually a minimum because tilt-blocking did not engulf the entire crater, but rather was constrained to a small area in its center, increasing the local strain there to over 50%. Both methods also reproduce the same relative order of ob served strain.

Our typical assumption was that the fault scarps were the light, "icy" halves of fault blocks. We tested this assumption by switching x and y, which drastically changed the strain results. For example, the strain in Crater A changed from 144% to 53% ± 26 under this assumption. Since the former number agrees with the crater measurement, we are confident that the light, icy halves of the fault blocks are indeed the fault scarps.

Another aspect of our results is that the fault geometry method yields strain values that are below the values found by Pappalardo and Collins. One possible explanation could be the effect of unobserved secondary faulting.

Because our geometric method is fairly simple and appears to adequately reproduce the magnitude of strain measured from strained craters, it will be applied to the rest of the surface of Ganymede to determine strain in more areas. These values will help in the future to estimate global strain, with implications for the internal evolution of the satellite.

References: [1] Pappalardo and Collins, *J. Struct. Geol.* 27, 827-838, 2005; [2] Collins et al., *GRL* 25, 233-236, 1998; [3] Pappalardo et al., *Icarus* 135, 276-302, 1998; [4] Giese et al., *LPSC XXXII*, #1751, 2001.

Area	Deformed crater [1]	Fault geom., θ = 45°	Fault geom., θ = 60°
Crater A	183% ± 68	144% ± 26	143% ± 26
Crater B	10.5% ± 4.5*	80% ± 17	67% ± 17
Crater C	107% ± 27	82% ± 20	68% ± 20
Crater D	15.3% ± 1.3	53% ± 18	34% ± 18
Crater E**	5.1% ± 0.5	4% ± 2	4% ± 2
Nicholson-Harpagia		49% ± 22	45% ±20

*minimum estimate, due to two sets of faults in crater, central strain much larger, see [1] **graben method

Table 1: Results of comparing fault geometry methods with strained crater measurements.